Forward diffraction amplitude of pp and $\bar{p}p$ elastic scattering at accelerator energies

M. Kawasaki*
Physics Department, Gifu University, Yanagido, Gifu 501-1193, Japan

T. Maehara†
Graduate School of Education, Hiroshima University, Higashi-Hiroshima 739-8524, Japan

M. Yonezawa‡
Nakano 7-5-28, Aki-ku, Hiroshima 739-0321, Japan
(Received 24 September 2004; published 15 December 2004)

A simple relation between the total cross section and the forward exponential slope of the elastic differential cross section of pp and $\bar{p}p$ scattering is indicated. An interpretation of this relation is presented as the formation of a black-disk structure for the elastic diffraction interaction of hadron-hadron scattering at the nonasymptotic energy region.

DOI: 10.1103/PhysRevD.70.114024 PACS numbers: 13.85.Dz, 12.40.Nn, 13.85.Lg

The diffraction interaction at small momentum transfers is the typical strong interaction in the soft region where nonperturbative effects are essential. The study of this interaction by QCD is, however, still on its way to the full explanation. For the momentum-transfer structure of the diffraction amplitude we have little theoretical understanding except that the amplitude will become that of the black-disk absorption asymptotically [1]. At the nonasymptotic region as the currently available accelerator energies, we do not know how the feature leading to the asymptotic structure is built. In this paper we show some simple relation between the total cross section and the forward exponential slope of the elastic differential cross section of hadron-hadron scattering, which seems to suggest the formation of a black-disk structure at nonasymptotic energies.

Conventionally the total cross section σ_t and the forward exponential slope B are plotted with respect to the total energy in the center of mass system $\sqrt{s}$. Different representation sometimes gives a new insight to the problem.

Here we assume the dominance of the exchange-even diffraction amplitude in the sense that we do not distinguish between pp and $\bar{p}p$ scattering. In Fig. 1 we show the forward slope B of the elastic differential cross section vs. the total cross section σ_t of pp and $\bar{p}p$ scattering in the energy region from the CERN Intersecting Storage Rings (ISR) to the Fermilab Tevatron Collider, through the CERN Super Proton Synchrotron ($Sp\bar{p}S$) [2–7]. As for the ISR experiments we have given in Fig. 1 only the experiments measuring both the total cross section and the forward slope, consistent with the present purpose [8].

The experimental data seem to lie along a line with sharp bend near the highest ISR energy point. Two line segments are to guide eyes. The first segment with steep slope is given by

$$B = -2.31(\pm 3.28) + 0.363(\pm 0.078)\sigma_t, \quad (1)$$

and the second segment by

$$B = 8.83(\pm 0.76) + 0.104(\pm 0.012)\sigma_t. \quad (2)$$

Here B is given in units of $(\mathrm{GeV}/c)^{-2}$ and σ_t in mb. The first segment is obtained for the ISR pp data set by the maximum likelihood method and the second one for the data set from the ISR top energy of pp at $\sqrt{s} = 62.8$ GeV to the Tevatron $\bar{p}p$ at 1800 GeV, assuming a linear formula $B = a + b\sigma_t$ [9].

The first segment indicates the relation $B \propto \sigma_t$, which is explained by the geometrical scaling (GS) [10], though its physical meaning is not clear. The slope of the second

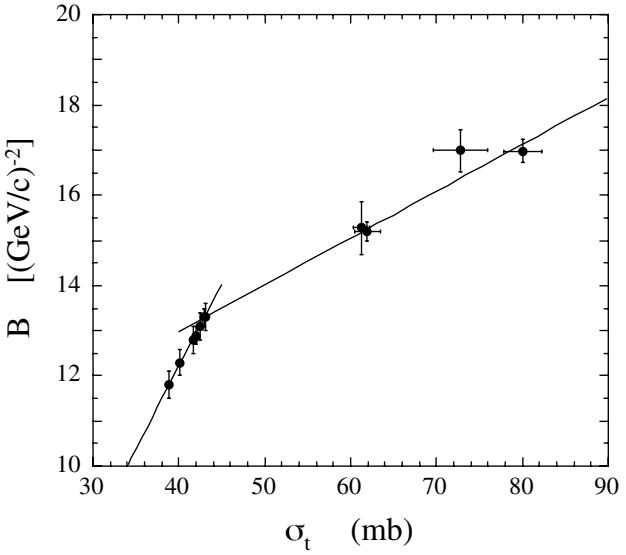

FIG. 1. The forward slope B of the elastic differential cross section vs the total cross section σ_t of pp and $\bar{p}p$ scattering.

*Electronic address: kawasaki@cc.gifu-u.ac.jp
†Electronic address: tmaehar@hiroshima-u.ac.jp
‡Electronic address: m-yonezawa@mtc.biglobe.ne.jp

segment is interestingly compared with the value of the asymptotic black-disk absorption $b = (1/8\pi) = 0.102\ \mathrm{mb}^{-1}(\mathrm{GeV}/c)^{-2}$. The implication of the second segment is our main concern in this paper with the view that this is not accidental.

Under the circumstances we take the following black-disk amplitude of the radius R with a form factor f for the imaginary part of the scattering amplitude F

$$\mathrm{Im}, F = R^2 \frac{J_1(Rq)}{Rq} f\left(\frac{q}{\lambda}\right), \tag{3}$$

where J_1 is the Bessel function of order 1, f some function of the momentum transfer q given by the squared momentum transfer t as $q = \sqrt{-t}$ with normalization $f(0) = 1$, R the black-disk radius, and λ the energy-dependent scale parameter of mass dimension.

This gives the forward slope

$$B = \frac{1}{8\pi}\sigma_{\mathrm{t}} + \frac{2}{\kappa^2} \quad \text{with} \quad \frac{1}{\kappa^2} \equiv -\left(\frac{1}{2q}\frac{df}{dq}\right)\Big|_{q=0}, \tag{4}$$

where σ_{t} is given by $2\pi R^2$ for the black-disk amplitude (3). The steep rise of B around $\sigma_{\mathrm{t}} = 40$ mb occurs in the ISR energy region, which is characterized by the relation $\kappa^2\sigma_{\mathrm{t}} = \tau$ with a constant τ. This gives the straight line

$$B = \left(\frac{1}{8\pi} + \frac{2}{\tau}\right)\sigma_{\mathrm{t}}, \tag{5}$$

which means the geometrical scaling. The amplitude (3) has the scaling property for $R\lambda =$ constant.

The next segment covers the wide energy region from the top energy of ISR to that of Tevatron and is specified by κ rather weakly varying with the energy. The values of κ estimated from B and σ_{t} by the formula (4) are 0.474, 0.475, and 0.467 GeV (the average of E-710 [6] and CDF [7]) at $\sqrt{s} = 62.5$, 540, and 1800 GeV, respectively, while the radius R increases by about 30% in this energy interval. Constancy of κ implies a straight line with slope $(1/8\pi)$.

Now the question is to what extent the black-disk picture (3) can describe the diffraction peak. The amplitude (3) has a zero at $Rq = 3.832...$ of J_1 producing the dip structure of the differential cross section around $|t| = 0.60\ (\mathrm{GeV}/c)^2$ for $\sigma_{\mathrm{t}} = 60$ mb, while the experiments of $\bar{p}p$ scattering seem to be consistent with a zero in $|t| \gtrsim 0.9\ (\mathrm{GeV}/c)^2$ at $\sqrt{s} = 546$ GeV. So we expect the formula will be applicable only in the region of small momentum transfer as $|t| \leq 0.2\ (\mathrm{GeV}/c)^2$. In order to examine the $|t|$-dependence of the form factor we evaluate it from the experimental data of the differential cross section [4,7,11,12] by fixing the value of R from the experimental data of the total cross section σ_{t} as $R = \sqrt{\sigma_{\mathrm{t}}/2\pi}$. The results are given in Fig. 2 for $\sqrt{s} = 62.5$, 546, and 1800 GeV, where the values of κ are approximately the same. Figure 2 shows a good degeneracy of the form factor at least in the momentum transfer $|t| \leq 0.2\ (\mathrm{GeV}/c)^2$.

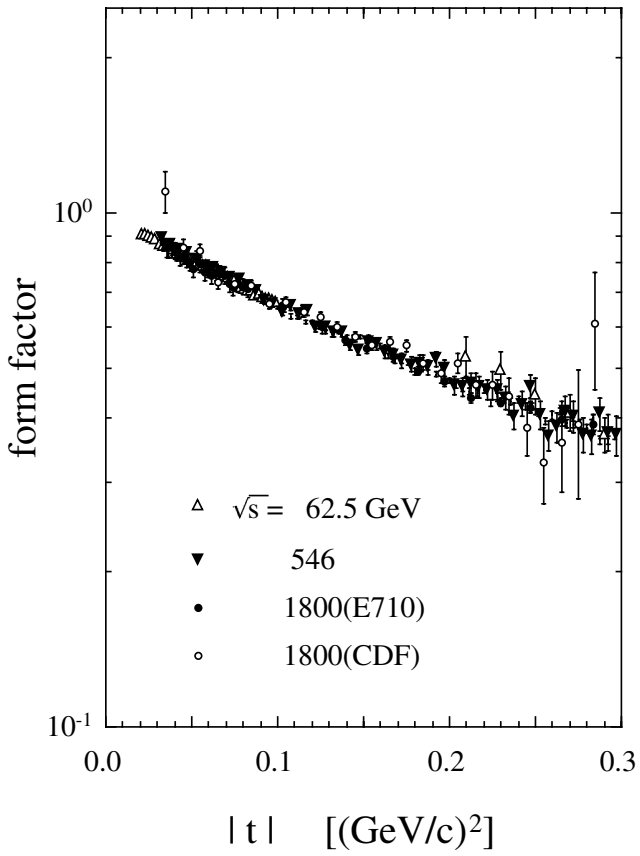

FIG. 2. The form factor evaluated from the experimental data at $\sqrt{s} = 62.5$, 546, and 1800 GeV.

It will be interesting to fit the differential cross section data directly by the amplitude (3) with a simple form factor. We test the following multipole form factor

$$f_{\mathrm{mp}} = \left(1 + \frac{q^2}{\lambda^2}\right)^{-n}. \tag{6}$$

The quantity λ is a parameter of mass dimension which gives $\kappa = \lambda/\sqrt{n}$ and n is the multiplicity of the pole, though we do not restrict it to the integer. For simplicity we assume n is independent of energy. Contributions from the real part of the scattering amplitude are neglected in the present analysis [13].

Varying the parameters R and λ for a fixed n in $1 \leq n \leq 2$ at each energy point, we have obtained the solutions by the χ^2-minimization fit to the differential cross section data only in the range of the momentum transfer $0.02 \leq |t| \leq 0.2\ (\mathrm{GeV}/c)^2$ from the experiments of Refs. [4,7,11,12]. Here the lower bound of $|t|$ is taken to avoid the effects of the Coulomb interaction. The feature of the fit to the experimental data is essentially unchanged for n between 1 and 2, with the best solution around 1.8. We give the results for $n = 1$ and 2 in Table I and for $n = 1$ in Fig. 3.

The agreement between the solutions and the experimental data is reasonably good, including the data in the

TABLE I. The results of the fit by the formula (3) with the form factor (6) to the experimental data of the differential cross section [4,7,11,12] for $n = 1$ and 2. The range of the momentum transfer of the experimental data taken in the fit is $0.02 \leq |t| \leq 0.2$ $(\mathrm{GeV}/c)^2$. Here N_{DP} is the number of the experimental data points. The numerical figures in the parentheses for σ_{t} and B are the experimental data.

	Process	$\sqrt{s}$ (GeV)	χ^2/N_{DP}	R $(\mathrm{GeV})^{-1}$	λ (GeV)	σ_{t} (mb)		B $(\mathrm{GeV}/c)^{-2}$	
$n = 1$	pp	23.5	35/40	4.06	0.438	40.25	(38.88 ± 0.21)	14.53	(11.8 ± 0.3)
	pp	30.7	80/63	4.09	0.454	40.91	(40.16 ± 0.22)	13.90	(12.3 ± 0.3)
	pp	44.7	176/89	4.17	0.426	42.63	(41.70 ± 0.21)	15.38	(12.8 ± 0.3)
	pp	52.8	109/61	4.24	0.423	43.98	(42.50 ± 0.27)	15.67	(13.1 ± 0.3)
	pp	62.5	71/40	4.25	0.437	44.09	(43.04 ± 0.31)	14.98	(13.3 ± 0.3)
	$\bar{p}p$	546	36/34	5.16	0.423	65.10	(61.9 ± 1.5)	17.83	(15.2 ± 0.2)
	$\bar{p}p$	(E-710)1800	23/32	5.55	0.425	75.44	(72.8 ± 3.1)	18.78	(16.99 ± 0.47)
	$\bar{p}p$	(CDF)1800	24/17	5.79	0.445	81.92	(80.03 ± 2.24)	18.48	(16.98 ± 0.25)
$n = 2$	pp	23.5	37/40	3.98	0.687	38.73	(38.88 ± 0.21)	12.43	(11.8 ± 0.3)
	pp	30.7	72/63	4.05	0.696	40.10	(40.16 ± 0.22)	12.36	(12.3 ± 0.3)
	pp	44.7	221/89	4.12	0.660	41.61	(41.70 ± 0.21)	13.45	(12.8 ± 0.3)
	pp	52.8	130/61	4.17	0.659	42.61	(42.50 ± 0.27)	13.56	(13.1 ± 0.3)
	pp	62.5	58/40	4.21	0.661	43.36	(43.04 ± 0.31)	13.60	(13.3 ± 0.3)
	$\bar{p}p$	546	41/34	5.08	0.653	63.24	(61.9 ± 1.5)	15.85	(15.2 ± 0.2)
	$\bar{p}p$	(E-710)1800	20/32	5.47	0.657	73.14	(72.8 ± 3.1)	16.75	(16.99 ± 0.47)
	$\bar{p}p$	(CDF)1800	25/17	5.68	0.683	78.94	(80.03 ± 2.24)	16.63	(16.98 ± 0.25)

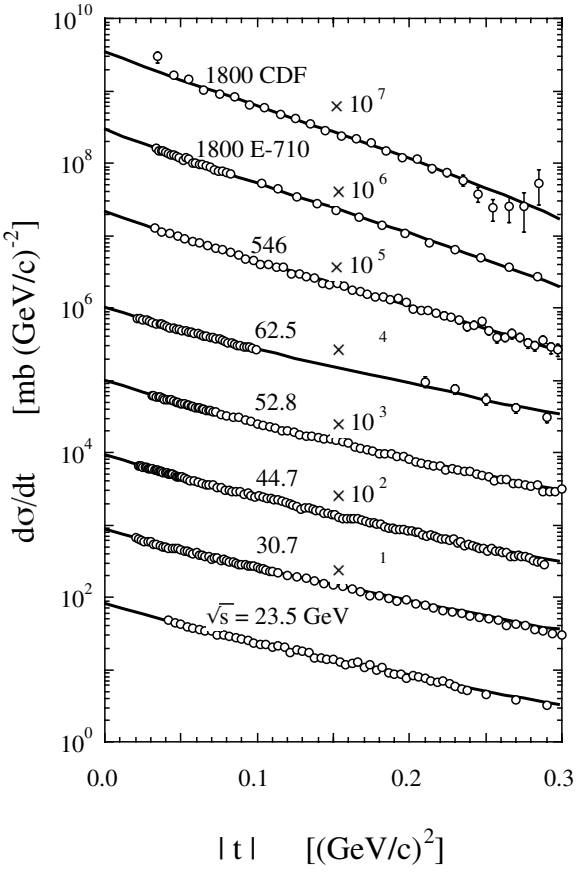

FIG. 3. The results of the fit to the differential cross sections by the formula (3) with the form factor (6) for $n = 1$. The experimental data are taken from Refs. [4,7,11,12].

range $0.2 \leq |t| \leq 0.3$ $(\mathrm{GeV}/c)^2$ not used in the fit. It is noted that the predicted values of σ_{t} and B for $n = 1$ given in Table I are systematically higher than the experimental ones. This is due to the curvature structure of the $n = 1$ amplitude, not negligible even in the small momentum transfer region $|t| \leq 0.02$ $(\mathrm{GeV}/c)^2$. For $n = 2$ this discrepancy virtually disappears. Another point to be emphasized is the approximate constancy of λ around from the top energy of ISR to Tevatron over a wide range of energy, as expected from the variation of κ. Roughly speaking there will be decrease in the value of λ with energy in the ISR region, but its change is not monotone and does not match the variation of R to produce a clear GS behavior as shown in Fig. 1. As the GS behavior of the ISR data is closely related to the bending feature of $\sigma_{\mathrm{t}} - B$ trajectory, we examine this problem next.

So far the analysis is *energy-independent*: we have searched the best-fit solution at each energy independently of other energy points, without seeking the continuation of the solutions with energy. To examine the compatibility of the present model with the ISR experimental data about the geometrical scaling, we have performed an *energy-dependent* analysis. By imposing the constraint $R\lambda =$ constant, we have made a fit to all of the data at five energy points [11] simultaneously, assuming $n = 2$. The results are given in Table II. Naturally the χ^2-values increase from the corresponding ones in Table I, particularly at $\sqrt{s} =$ 44.7 and 30.7 GeV, but the results show that the present diffraction amplitude has the solutions consistent with the ISR experimental data about the GS hypothesis.

Theoretical support for the amplitude (3) can be obtained by the Regge-pole approach [14] or the eikonal approach [15]. In particular, the latter gives the explicit

TABLE II. The results of the compatibility test for the geometrical scaling. The ISR pp experimental data of the differential cross section taken in Table I are fitted simultaneously by the formula (3) with the form factor (6) for $n = 2$ under the constraint $R\lambda =$ constant.

$\sqrt{s}$ (GeV)	χ^2/N_{DP}	R (GeV)$^{-1}$	λ (GeV)
23.5	38/40	3.95	0.695
30.7	136/63	4.07	0.676
44.7	265/89	4.11	0.670
52.8	130/61	4.17	0.660
62.5	69/40	4.22	0.652

expression for the form factor as

$$f_{\mathrm{asy}} = \mathrm{Re}, \Gamma\left(1 + i\frac{q}{\mu}\right), \tag{7}$$

where Γ is the gamma function and the mass parameter μ specifies the most peripheral part of the diffraction interaction in the impact-parameter space. This is derived by the asymptotic expansion and the amplitude (3) with the form factor (7) gives the leading term at small momentum transfers at very high energy. For the form factor (7) we have $\kappa^2 = 12\mu^2/(6\gamma^2 + \pi^2) = 0.989\mu^2$ where γ is the Euler constant.

The validity of the expression (7) holds strictly only asymptotically. It will be, however, reasonable to expect that the form factor f represents the peripheral part of the diffraction interaction also at the nonasymptotic energy region, at least, approximately. The form factor (7) is well simulated by a multipole one with $n = 1.16$ and $\lambda = 1.02\mu$ for $0 \leq |t|/\mu^2 \leq 2$ with deviation less than 1%. The results for the multipole $n = 1$ can be taken approximately as the ones for the form factor (7). The most peripheral part of the diffraction interaction is expected to be given by the two-pion continuum. The value of μ will fall in the range 0.42–0.51 GeV from the values of λ in Table I and of κ evaluated by the experimental data of σ_{t} and B. This certainly suggests the dominance of two-pion mass states which are bounded from below by the threshold mass of 0.28 GeV.

As for the case $n = 2$ we have no reasonable way to associate the value of λ with hadron mass spectra, nor with matter distributions in the quark-gluon system. For $n = 2$, λ takes the value in 0.65–0.70 GeV, which is notably lower than 0.84 GeV of the mass of the proton electromagnetic dipole form factor. The present λ is near 0.73 GeV of the mass of the dipole taken for the gluonic distribution in the QCD-inspired model of Block *et al.* [16], although these two mass parameters appear in very different contexts. It will be interesting to observe how n and λ change with the energy.

Association of the asymptotic feature of the scattering amplitude with the structure of the forward amplitude in the accelerator energy region might be taken to be farfetched, as the slope $1/8\pi$ is only attained at very high energies for almost all the eikonal models so far proposed. The results of the analysis, however, seem to support the conjecture. As for the effects of nonleading terms in the asymptotic expansion, these will be certainly required if we go to larger momentum transfer region including the dip and beyond [17]. We have made an attempt to have a coherent understanding of diffraction interaction in the entire region of the momentum transfer where the experiments have been performed, by including some nonleading term in addition to the leading term (3). The consequences of the analysis are good qualitatively, but not satisfactory quantitatively [18].

We comment on the break structure of the slope of $\sigma_{\mathrm{t}} - B$ curve in Fig. 1 suggested earlier at the beginning of this paper. If this breaking behavior is *hard*, theoretical models will need some almost discrete changes in their diffraction components around the breaking point. All the theoretical models, as far as we know, give soft behavior for $\sigma_{\mathrm{t}} - B$ curve around the ISR highest energy end. As an example, we show the predictions of the QCD-inspired model [16] in Fig. 4. If the geometrical scaling holds very approximately as the QCD-inspired model shows, then we have a smooth change from ISR to higher energy. If, on the other hand, the geometrical scaling is as good as the ISR data, then the ISR results are difficult to be continued monotonous to the S$p\bar{p}$S and Tevatron data: we need either breaking structure or even oscillatory behavior in the energy region from ISR to Tevatron.

Future experiments at the BNL Relativistic Heavy Ion Collider (RHIC) and CERN Large Hadron Collider (LHC)

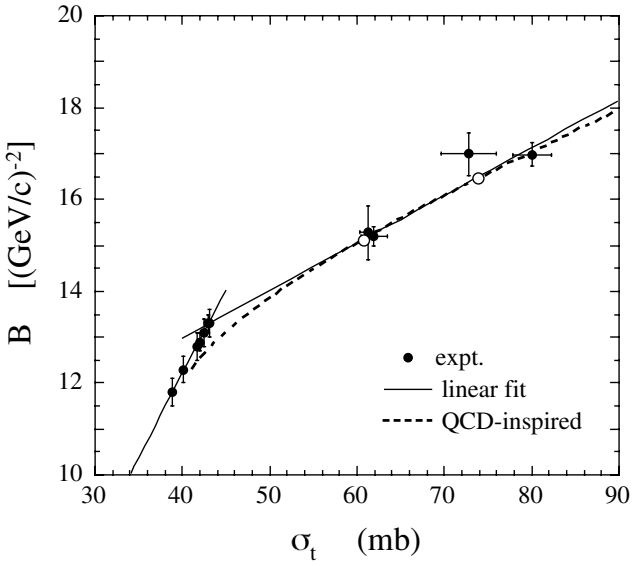

FIG. 4. The $\sigma_{\mathrm{t}} - B$ curve of the QCD-inspired model of Block *et al.* [16] and the experimental data. The open circles are the predictions of the model at $\sqrt{s} = 546$ and 1800 GeV.

will produce many valuable data for the diffraction of pp interaction. The pp2pp experiment at RHIC to measure polarized elastic pp scattering in the energy region $50 \leq \sqrt{s} \leq 500$ GeV is now in progress [19]. The low-energy end of this project overlaps with the ISR region and the project helps to build a comprehensive picture of pp scattering in the energy region $\sqrt{s} \leq 500$ GeV, filling the large gap between ISR and S$p\bar{p}$S. Experiments at LHC will provide us the information of pp interaction at the highest energy now accessible by accelerators where the diffraction interaction will show its feature more clearly [20].

[1] G. Auberson, T. Kinoshita, and A. Martin, Phys. Rev. D **3**, 3185 (1971).

[2] U. Amaldi *et al.*, Phys. Lett. **62B**, 460 (1976); L. Baksay *et al.*, Nucl. Phys. **B141**, 1 (1978).The numerical data of these experiments are taken from Ref. [3].

[3] K. R. Schubert, in *Elastic and Charge Exchange Scattering of Elementary Particles*, edited by H. Schopper and Landolt-Börnstein, New Series Vol. I/9a (Springer-Verlag, New York, 1980).

[4] UA4 Collaboration, M. Bozzo *et al.*, Phys. Lett. **147B**, 385 (1984).

[5] UA4 Collaboration, M. Bozzo *et al.*, Phys. Lett. **147B**, 392 (1984).

[6] E-710 Collaboration, N. A. Amos *et al.*, Phys. Rev. Lett. **68**, 2433 (1992).

[7] CDF Collaboration, F. Abe *et al.*, Phys. Rev. D **50**, 5518 (1994); **50**, 5550 (1994). The numerical data of this experiment is taken from http://durpdg.dur.ac.uk/HEPDATA/REAC.

[8] This choice for the data selection is not essential for the bending behavior of σ_{t}–B curve. If we include the rest of the data for B by taking σ_{t} of the empirical formula, the breaking feature of the slope is even more emphasized.

[9] At $\sqrt{s} = 1800$ GeV of the Tevatron energy, the value of the total cross section differs among the experiments. The CDF experiment gives $\sigma_t = 80.03 \pm 2.24$ mb, while E-710 gives 72.8 ± 3.1 mb and the recent E-811 is consistent with E-710 giving 71.71 ± 2.02 mb; E-811 Collaboration, C. Avila *et al.*, Phys. Lett. B **445**, 419 (1999).These results appear as fairly separated points in the Fig. 1 and makes the $\sigma_{\mathrm{t}} - B$ trajectory uncertain. We have not given the E-811 data in Fig. 1 as the value of B is assumed in this experiment.

[10] J. Dias de Deus, Nucl. Phys. **B59**, 231 (1973); A. J. Buras and J. Dias de Deus, *ibid.* **B71**, 481 (1974).

[11] G. Barbiellini *et al.*, Phys. Lett. **39B**, 663 (1972); U. Amaldi *et al.*, Phys. Lett. **66B**, 390 (1977); L. Baksay *et al.*, Nucl. Phys. **B141**, 1 (1978). The numerical data of these experiments are taken from Ref. [3].

[12] E-710 Collaboration, N. A. Amos *et al.*, Phys. Lett. B **247**, 127 (1990).The numerical data of this experiment is taken from http://durpdg.dur.ac.uk/HEPDATA/REAC .

[13] The contribution from the real part is essential if we involve the Coulomb interference region or the dip region in the analysis. The real part may be included either by simply multiplying $(1 - i\rho)$ factor to the imaginary part where ρ is the ratio of the real to the imaginary part of the forward scattering amplitude, or, more elaborately, by the derivative dispersion relation.For the derivative dispersion relation see J. B. Bronzan, G. L. Kane, and U. P. Sukhatme, Phys. Lett. **49B**, 272 (1974); J. D. Jackson, in *Proceedings of Fourteenth Scottish Universities Summer School in Physics, 1973*, edited by R. L. Crawford and R. Jennings (Academic Press, London, 1974), p. 1.

[14] P. Gauron, B. Nicolescu, and E. Leader, Nucl. Phys. **B299**, 640 (1988).

[15] M. Kawasaki, T. Maehara, and M. Yonezawa, Phys. Rev. D **62**, 074005 (2000).

[16] M. Block, R. Fletcher, F. Halzen, B. Margolis, and P. Valin, Phys. Rev. D **41**, 978 (1990).

[17] M. Kawasaki, T. Maehara, and M. Yonezawa, Phys. Rev. D **67**, 014013 (2003).

[18] M. Kawasaki, T. Maehara, and M. Yonezawa, Mod. Phys. Lett. A **19**, 3001 (2004).

[19] A recent RHIC pp2pp report gives the forward slope $B = 16.3 \pm 1.6(\mathrm{stat.}) \pm 0.9(\mathrm{syst.})$ $(\mathrm{GeV}/c)^{-2}$ at $\sqrt{s} =$ 200 GeV as a preliminary value; S. Bültmann *et al.*, Phys. Lett. B **579**, 245 (2004).Its central value is considerably larger than the interpolated value from previous experimental data. We have not shown this data as the total cross section was not measured by the experiment.

[20] Incidentally, the linear formula (2) gives $B = 20.48 \pm 0.63$ $(\mathrm{GeV}/c)^{-2}$ at the LHC energy $\sqrt{s} = 14$ TeV for $\sigma_{\mathrm{t}} = 111.7$ mb of the empirical formula for the total cross section.Particle Data Group, S. Eidelman *et al.*, Phys. Lett. B **592**, 1 (2004).It also gives $B = 14.24 \pm 0.19$ $(\mathrm{GeV}/c)^{-2}$ at $\sqrt{s} = 200$ GeV for $\sigma_{\mathrm{t}} = 51.78$ mb. This is compared with the RHIC value in Ref. [19].